Antennas on dielectric coated convex surfaces : theory and experimentation

M.-A. BLONDEEL-FOURNIER*, W. TABBARA** and L. BEAULIEU*

* Dassault Electronique
55, quai Marcel Dassault, 92214 Saint-Cloud cedex France.
** Laboratoire de Signaux et Systèmes
E.S.E. -C.N.R.S.
Plateau du moulon, 91192 Gif sur yvette cedex France.

1. Introduction

The purpose of this paper is to analyze the diffraction phenomenon introduced by perfectly conducting convex surfaces with dielectric coating, resulting from an interaction of these structures with an electromagnetic radiation created essentially by sources which are set on these objects at high frequencies, in other words for characteristic dimensions of the structures large in terms of wave-length.

When the object is perfectly conducting and of simple shape (sphere, cylinder, ellipsoid), analytic solutions can be obtained. These are eigenfunction series which converge slowly when the dimensions of the object become large in terms of wave-length. It is then necessary to develop asymptotic expressions from these exact solutions. A well known approach uses the Geometrical Theory of Diffraction (G.T.D.) and its extensions such as the Uniform Theory of Diffraction. We shall apply these methods to conducting structures with dielectric coating on which one or several sources like apertures or microstrip antennas are placed. We will primarily focus on the fields in the shadow region.

The case of cylinders with dielectric coating or surface impedance has received attention in the 1950's (for example Wait [12], Fock [2], Logan [7]). The purpose was to analyze the propagation of radio waves around the earth. In 1980, Rao and Hamid have given a geometrical interpretation of the diffraction phenomenon by a dielectric coated circular cylinder [10]. From the exact solution in the case of an infinite line source in presence of a circular cylinder with dielectric coating, the reflection and transmission coefficients are developed and a ray-optical approach is presented. It is essentially a qualitative analysis. As to Wang [13], he obtains the roots of the characteristic equation which describes the modes likely to propagate in the shadow region. Paknys [8] studies the surface field created by a magnetic or electric line set on a perfectly conducting circular cylinder with a dielectric coating. He develops the exact solution in the form of Hankel functions series and, by Watson's transformation and application of residues theorem, gives an asymptotic solution in form of residues. In 1986, Kim [5] completes the study by analysing the diffracted field due to an infinite line source in front of an infinite perfectly conducting cylinder with a dielectric coating. He studies the problem of a perfectly conducting circular cylinder with dielectric coating or impedance surface and develops the exact solution given as Hankel functions' series. From this solution, an asymptotic expansion is deduced in the lit region, the shadow region and the transition region. Pearson, in 1987, studies the 3 dimensional problem : radiation of an electric or a magnetic dipole in front of or on an infinite circular cylinder with dielectric coating [9]. Few experimental results are presented in the above contributions. In the present work, we first present the case of a source placed on a coated circular cylinder. The source is either a slot or a patch, and in the former case we compare the infinite line and the magnetic dipole models of the slot. This comparison shows how useful a 2D model can be in the analysis of a 3D problem. In a second step, we extend the circular cylinder solution to the case of a smooth convex surface. Here, at each point along a ray-path we approximate the convex surface by a circular cylinder having the same radius of curvature. The

theoritical results are established and applied to the cases of an elliptical cylinder and of a truncated cone. Since exact solutions are difficult to obtain in most cases, we checked our numerical results by comparing them to measured values of the radiated far-field, the surface field and the coupling coefficient of two slots.

In the following, the time dependance is assumed to be exp(jωt).

2. Radiation

2.1 Circular cylinder with dielectric coating

a) Dipole

The geometry of the problem is given in (Figure 1). The perfectly conducting infinite circular cylinder of radius a is coated by a homogeneous dielectric of relative complex permittivity ε_r ($\varepsilon_r = \varepsilon'_r - j\varepsilon''_r$). The thickness of the dielectric is d=b-a with b the outer radius of the coated cylinder. We note k_0 the free-space wave number.

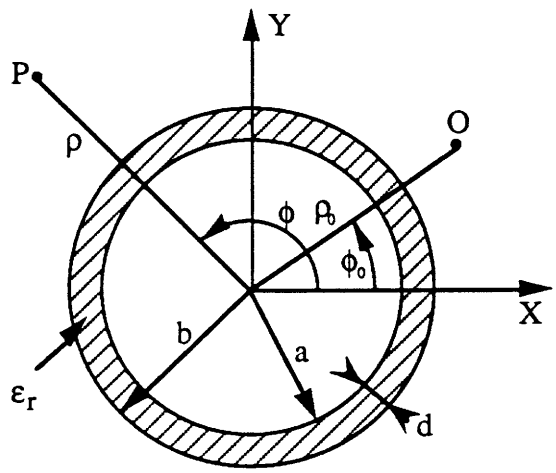

Figure 1 : dielectric coated cylinder

Cylindrical coordinates (ρ,ϕ,z) are used. At the point O, the source is a magnetic or electric dipole arbitrarily oriented with respect to the circular cylinder (3 dimensional problem). The position of the source is determined by $\vec{\rho_0}$ (ρ_0,ϕ_0,z_0) and that of the observation point P by $\vec{\rho}$ (ρ,ϕ,z). The electric and magnetic fields are given by :

$$\mathbf{E} = -\frac{1}{\omega\varepsilon}\,\mathrm{grad}(\mathbf{I}\cdot\mathrm{grad}G) - j\omega\mu(\mathbf{I}\cdot G) + \mathbf{K}\wedge\mathrm{grad}G$$

$$\mathbf{H} = -\frac{1}{\omega\mu}\,\mathrm{grad}(\mathbf{K}\cdot\mathrm{grad}G) - j\omega\varepsilon(\mathbf{K}\cdot G) + \mathbf{I}\wedge\mathrm{grad}G$$

where **K** and **I** are respectively the magnetic and the electric current densities and G a scalar Green's function.

When the source O and the field point P are outside the dielectric, the scalar Green's function in the TE case is given by the integral expression (5.1) in the appendix (for more complete theoretical developments see [1]). This Green's function is modified by Watson's transformation and then, approximated by application of the residues theorem. This leads to asymptotic

expressions valid only in the shadow region as defined by geometrical optic. The asymptotic expression of the Green's function takes the following form :

$$G \approx \frac{1}{8} \sum_{n=1}^{+\infty} \sum_{p=-\infty}^{+\infty} \int_{-\infty}^{+\infty} R_n(h)\, H_{\gamma_n}^{(2)}(v\rho)\, H_{\gamma_n}^{(2)}(v\rho_o)\, e^{-j\gamma_n|\phi - \phi_o| + 2\pi p)}\, e^{-jh(z-z_o)}\, dh \qquad (2.1)$$

where $R_n(h) = \dfrac{H_{\gamma_n}^{(1)\prime}(vb) - j\, C_h(\gamma_n) H_{\gamma_n}^{(1)}(vb)}{\left(\dfrac{\partial H_{\gamma}^{(2)\prime}(vb) - j\, C_h(\gamma) H_{\gamma}^{(2)}(vb)}{\partial \gamma}\right)_{\gamma = \gamma_n}}$ and $v^2 = k_o^2 - h^2$

The complex value γ_n is the n^{th} root of the characteristic equation :

$$H_{\gamma_n}^{(2)\prime}(vb) - j\, C_h(\gamma_n) H_{\gamma_n}^{(2)}(vb) = 0 \qquad (2.2)$$

The integral with respect to h is then approximated by replacing the Hankel functions by their Debye expansions which are valid for $\left|\frac{\gamma_n}{v\rho}\right| << 1$ and $\left|\frac{\gamma_n}{v\rho_o}\right| << 1$ [5] :

$$H_{\gamma_n}^{(2)}(v\rho) = \sqrt{\frac{2}{\pi v \rho \sin(\alpha)}}\, e^{-j(v\rho\sin(\alpha) - \alpha\gamma_n - \frac{\pi}{4})}$$

$$H_{\gamma_n}^{(2)}(v\rho_o) = \sqrt{\frac{2}{\pi v \rho_o \sin(\beta)}}\, e^{-j(v\rho_o\sin(\beta) - \beta\gamma_n - \frac{\pi}{4})}$$

where α and β are such that $\gamma_n = v\rho\cos(\alpha) = v\rho_o\cos(\beta)$.

We then introduce the effective radius of the cylinder called a_n slightly superior to b : $\gamma_n = \upsilon a_n - j a_n \delta_n$.

So α and β are now written as : $\alpha = \cos^{-1}\left(\frac{\gamma_n}{v\rho}\right) \approx \cos^{-1}\left(\frac{a_n}{\rho}\right)$ $\beta = \cos^{-1}\left(\frac{\gamma_n}{v\rho_o}\right) \approx \cos^{-1}\left(\frac{a_n}{\rho_o}\right)$

This permits to consider the parameter $\sigma_n = |\phi - \phi_o| + 2\pi p - \cos^{-1}\left(\frac{a_n}{\rho}\right) - \cos^{-1}\left(\frac{a_n}{\rho_o}\right)$ as an angular distance. Therefore, (2.1) reduces to :

$$G \approx \frac{j}{4\pi} \sum_{n=1}^{+\infty} \sum_{p=-\infty}^{+\infty} \int_{-\infty}^{+\infty} R_n(h) \sqrt{\frac{1}{v\sqrt{\rho^2 - a_n^2}\, v\sqrt{\rho_o^2 - a_n^2}}}$$

$$e^{-j(h(z-z_o) + \gamma_n\sigma_n + v\sqrt{\rho - a_n^2} + v\sqrt{\rho_o - a_n^2})}\, dh \qquad (2.3)$$

The exponential term of the scalar Green's function is now written as : $e^{-jh(z-z_o)-j\nu l_n-a_n\delta_n\sigma_n}$

where $l_n=\sqrt{\rho^2-a_n^2}+\sqrt{\rho_o^2-a_n^2}+a_n\sigma_n$, in order to apply the stationary phase method to the integral with respect to h. We set

$$\theta_n=\tan^{-1}\left(\frac{L_n}{z-z_o}\right) \text{ and } L_n=\sqrt{l_n^2+(z-z_o)^2}$$

$$l_n=L_n\sin(\theta_n) \text{ and } (z-z_o)=L_n\cos(\theta_n) \qquad h=k_o\cos T \text{ and } \nu=k_o\sin T$$

This method of approximation is presented in [9] and leads to :

$$G\approx G_o(Q_1)\sum_{n=1}^{+\infty}\sum_{p=-\infty}^{+\infty}D_n^h(Q_1)\,e^{-j\gamma_n\sigma_n\sin\theta_n}\sqrt{\frac{S_1}{L_nS_2}}D_n^h(Q_2)\,e^{-jk_oS_2} \qquad (2.4)$$

where

$\sqrt{\rho_o^2-a_n^2}=S_1\sin\theta_n$ and $\sqrt{\rho^2-a_n^2}=S_2\sin\theta_n$

$G_o(Q_1)=\frac{-1}{4\pi}\frac{e^{-jk_oS_1}}{S_1}$ is the free-space Green's function

$$\left[D_n^h(Q)\right]^2=\frac{j}{\sin\theta_n}\sqrt{\frac{2\pi j}{k_o}}\frac{H_{\gamma_n}^{(1)\prime}(k_obsin\theta_n)-j\,C_h(\gamma_n)H_{\gamma_n}^{(1)}(k_obsin\theta_n)}{\left(\frac{\partial\left[H_\gamma^{(2)\prime}(k_obsin\theta_n)-j\,C_h(\gamma)H_\gamma^{(2)}(k_obsin\theta_n)\right]}{\partial\gamma}\right)_{\gamma=\gamma_n}} \qquad (2.5)$$

$e^{-j\gamma_n\sigma_n\sin\theta_n}$ caracterizes the creeping wave attenuation on the dielectric coating.

Referring to the studies in the case of a perfectly conducting convex surface, we consider two points on the dielectric surface called Q_1 and Q_2. The incident ray (OQ_1) hits the dielectric surface tangentially at Q_1, creating a creeping wave which propagates along an arc of geodesic on the dielectric surface (Q_1Q_2). This type of waves propagates with an exponential attenuation. (Figure 2) gives a geometrical interpretation of this problem. S_1 is the distance OQ_1, S_2 the distance Q_2P.

The complex number γ_n represents the propagation constant of the creeping waves on the dielectric coating. The index p defines the number of encirclements done by the creeping ray on the coating. In general, one mode of the creeping waves (n=1) and two associated rays (p=0 and p=-1) are sufficient to describe the phenomenon if the dielectric thickness is $\leq 0.1\,\lambda$.

When the source is inside the dielectric, the scalar Green's function is given by (5.3) presented in the appendix. This function is approximated by application of the residues theorem and the Watson's transformation. Unlike the case of a source located outside the dielectric, the Debye developments of the Hankel functions cannot be used. So, we must define new coefficients homogeneous to the classic diffraction coefficients developed in the first part.

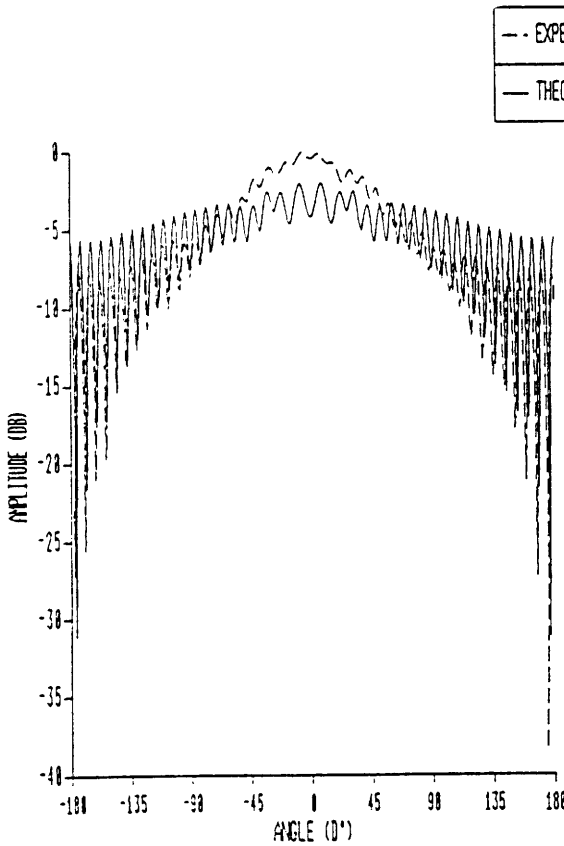

Figure 4 : slot modelled by a dipole

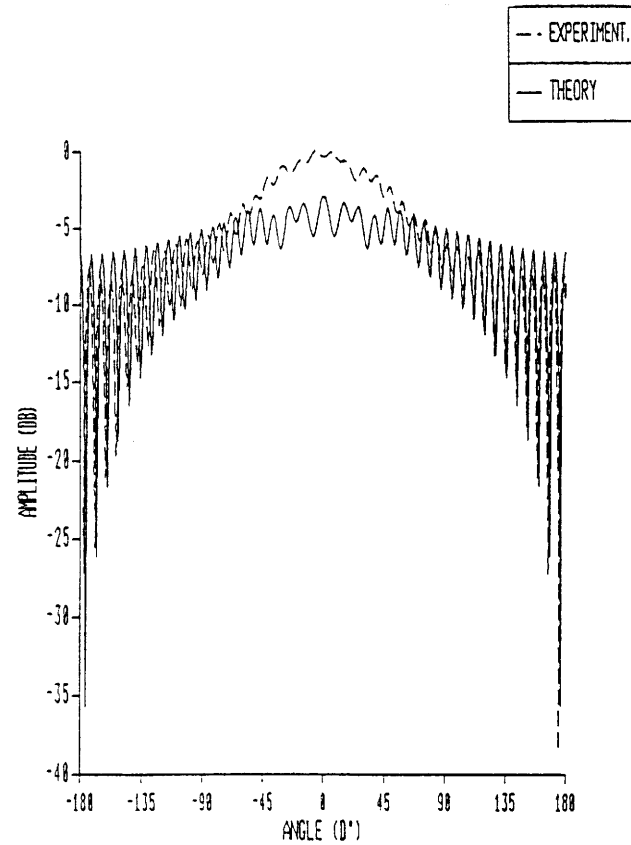

Figure 5 : slot modelled by a line

2.2 Smooth convex surface with dielectric coating

a) Theory

For a dielectric coated convex surface of arbitrary shape and one infinite radius of curvature, the paths of the rays are obtained by assuming that at each point, the surface behaves like a coated circular cylinder whose radius of curvature is equal to that of the surface at this point. In the following, we present very briefly the main points in the process of extending the results of the circular cylinder to a convex surface.

The radius ρ_1 denotes the curvature in a direction defined by the vector multiplication of the principal vector following the generating lines with the vector supported by the normal.

Then, the Green's function is obtained from the one relative to the circular cylinder :

$$G(P) \approx G_o(Q_1)\, T_h \sqrt{\frac{\rho_2^d}{S_2\left(\rho_2^d + S_2\right)}}\, e^{-jk_oS_2} \qquad (2.8)$$

$$T_h = \sum_{p=1}^{N} D_p^h(Q_1) \left(e \int_{Q_1}^{Q_2} -j\gamma_n(t')\sin\theta_n dt' \sqrt{\frac{d\eta(Q_1)}{d\eta(Q_2)}} \right) D_p^h(Q_2)$$

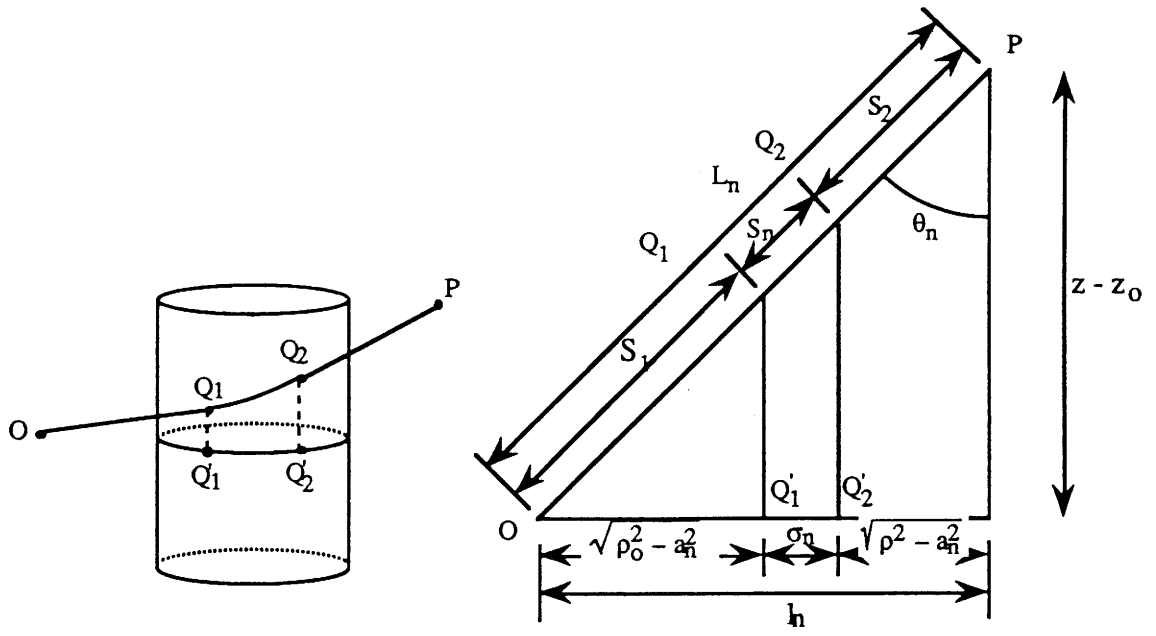

Figure 2 : creeping waves on the dielectric surface

b) Line

A simplified model of the slot is realized by means of a magnetic longitudinal infinite line parallel to the generating lines of the circular cylinder. The problem becomes bidimensionnal and is solved as in the 3 dimensional case (dipole source). According to [1], the asymptotic expression of the Green's function is given by (using the same notations as in the 3D case) :

$$G \approx G_o(Q_1) \sum_{n=1}^{\infty} \sum_{p=-\infty}^{+\infty} \left\{ D_n^h(Q_1)\, e^{-j\gamma_n \sigma_n}\, D_n^h(Q_2) \right\} \frac{e^{-jk_o S_2}}{\sqrt{S_2}} \qquad (2.6)$$

where $G_o(Q_1) = \dfrac{e^{-j\pi/4}}{2\sqrt{2\pi}} \dfrac{e^{-jk_o S_1}}{\sqrt{k_o S_1}}$ (free-space Green's function),

$\left[D_n^h(Q)\right]^2 = j\sqrt{\dfrac{2\pi j}{k_o}} \dfrac{H_{\gamma_n}^{(1)\prime}(k_o b) - j\, C_h(\gamma_n) H_{\gamma_n}^{(1)}(k_o b)}{\left(\dfrac{\partial \left[H_\gamma^{(2)\prime}(k_o b) - j\, C_h(\gamma) H_\gamma^{(2)}(k_o b) \right]}{\partial \gamma} \right)_{\gamma = \gamma_n}}$ defines the diffraction coefficient at Q_1 and Q_2 ,

S_1 and S_2 represent respectively the distances source point O- diffraction point Q_1 and diffraction point Q_2 - field point P, σ_n is the angular distance separating the two diffraction points and γ_n the n^{th} root of the characteristic equation :

$$H_{\gamma_n}^{(2)\prime}(k_o b) - j\, C_h(\gamma_n) H_{\gamma_n}^{(2)}(k_o b) = 0 \qquad (2.7)$$

The roots of the characteristic equations (2.2) and (2.7) are determined with an accuracy of 10^{-3}. For errors up to 10^{-2}, there is no noticeable change in the accuracy of the final result.

c) Patch on a dielectic coated circular cylinder

The microstrip patch is set on the perfectly conducting surface of a circular or elliptic cylinder with dielectric coating. Simple models like the transmission line or the cavity ones give satisfactory results for the far-field radiation pattern from a microstrip patch antenna set on a planar surface or on a perfectly conducting circular cylinder [11]. Recently, the theoretical radiation pattern of a square patch tilted by 45° with respect to the generating lines of the perfectly conducting circular cylinder has been compared with the experimental one [4]. We apply the cavity model to a tilted microstrip patch placed on a coated circular cylinder.

According to the cavity model, the patch can be replaced by four slots. Two slots (1 and 2) are excited by a constant current and two slots (3 and 4) by a simple cosine distribution (Figure 3). The length of the slot is equal to the side length of the square (a = 9.36 mm) and this width to the dielectric thickness (d = 3mm). So, the total radiation field is the vector sum of the fields radiated by each slot. The working frequency is 8 GH_z.

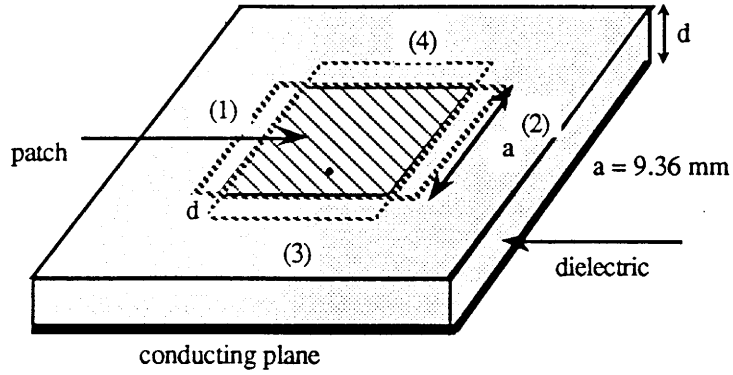

Figure 3 : patch and its equivalent slots

d) Experimentation

The first results present the radiation pattern of a slot on a cylinder. An X-band slot is set on the conducting surface of a perfectly conducting circular cylinder of radius a=95mm, with a dielectric coating of thickness d=3mm and permittivity ε_r = (2.59,-0.02). The results are given at a frequency of 10 GH_z. (Figure 4) shows the equatorial radiation far-field pattern of the slot modelled by a dipole whereas those related to the infinite magnetic line are reported on (Figure 5). The thickness of the dielectric is equal to 0.1λ : one mode and the two associated rays are sufficient for the computation of the far-field.

Whatever the source model, the oscillations of the theoretical field are in agreement with the ones observed in the experimentation except in the vicinity of the source. In the shadow region, the relative levels are correct. The modelization of the slot by a line source gives good results, this is an interesting model because it is a 2 dimensional one, easy to use and which gives a good interpretation of the physical phenomenons.

The radiation pattern of a microstrip patch (with the same ε_r as above) is given in (Figure 6). By comparison with the case of an uncoated perfectly conducting cylinder [4], the presence of a dielectric modifies the far-field radiation patterns : the E_θ component is much less attenuated than in the case of a perfectly conducting cylinder. The creeping waves are guided on the dielectric surface. Consequently, the losses relative to the radius of curvature are reduced. The experimental and theoretical results of the component E_ϕ compare favorably for $\phi \leq 120°$.

Q_1 and Q_2 are the diffraction points on the dielectric surface. S_2 is the distance diffraction point Q_2 - field point P.

Diffraction coefficients :

So, the diffraction coefficient is given by :

$$\left[D_n^h(Q)\right]^2 = \frac{j}{\sin\theta_n}\sqrt{\frac{2\pi j}{k_o}}\frac{H_{\gamma_n}^{(1)\prime}(k_o\rho_1\sin\theta_n) - j\,C_h(\gamma_n)\,H_{\gamma}^{(1)}(k_o\rho_1\sin\theta_n)}{\left(\frac{\partial\left[H_{\gamma}^{(2)\prime}(k_o\rho_1\sin\theta_n) - j\,C_h(\gamma)\,H_{\gamma}^{(2)}(k_o\rho_1\sin\theta_n)\right]}{\partial\gamma}\right)_{\gamma=\gamma_n}} \quad (2.9)$$

The angle θ_n is defined as in the case of a circular cylinder with the help of the paths introduced for each ray. And γ_n is the n^{th} root of the modified characteristic equation :

$$H_{\gamma}^{(2)\prime}(k_o\rho_1\sin\theta_n) - j\,C_h(\gamma)\,H_{\gamma}^{(2)}(k_o\rho_1\sin\theta_n) = 0 \quad (2.10)$$

When the surface is convex, the radius of curvature at Q_1 and Q_2 are different. Consequently, the roots of the characteristic equation (or the poles-residues) depend on the radius of curvature and must be calculated for each point of diffraction.

Creeping wave attenuation :

Before, the exponential term associated with the creeping wave has been decomposed in two terms : a term of phase given by the arc length and a term of attenuation. Now, the pole-residue depend on the radius of curvature of each point of diffraction. Thus, we shall write the exponentional term as : $e^{\int_{Q_1}^{Q_2} -j\gamma_n\sin\theta_n dt'}$ where dt' is an elementary arc length.

Divergence factor :

The convex surface considered here are developable, thus the divergence factors $\sqrt{\frac{d\eta(Q_1)}{d\eta(Q_2)}}$ and $\sqrt{\frac{\rho_2^d}{s_2\left(\rho_2^d + s_2\right)}}$ are computed similarly to those in the case of uncoated perfectly conducting convex surfaces [1].

b) Experimentation

At mid-height of a perfectly conducting truncated circular cone of half-angle 7.76° and height h=300mm (radius of the larger base r_{max}=129.65mm and that of the smaller base r_{min}=70.35mm), an X-band slot is set on the conducting surface. The coating has a dielectric thickness d=3mm and permittivity ε_r = (3.4,-0.1). The radiation pattern $|E_\Phi|$ is computed at 10GH$_z$. (Figure 7) shows the equatorial far-field radiation pattern (θ=90°) of the slot modelled by a magnetic dipole. The thickness of the dielectric is 0.1λ : one mode and the two associated creeping waves are considered.

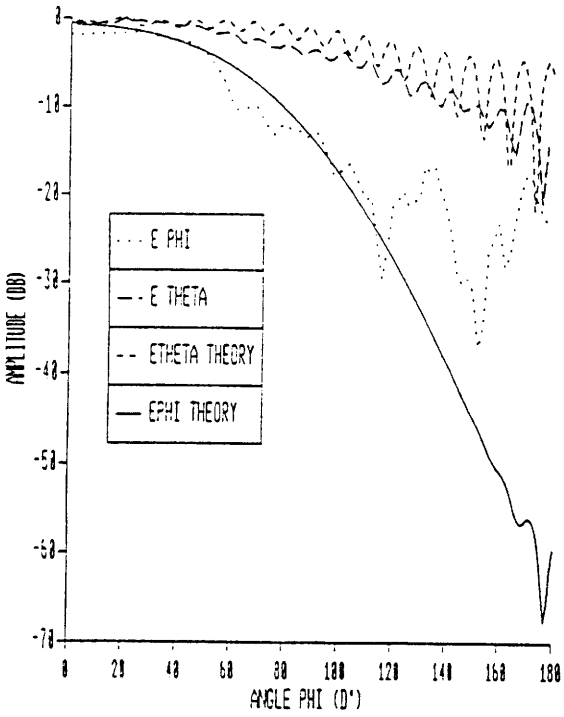

Figure 6 : tilted microstrip patch

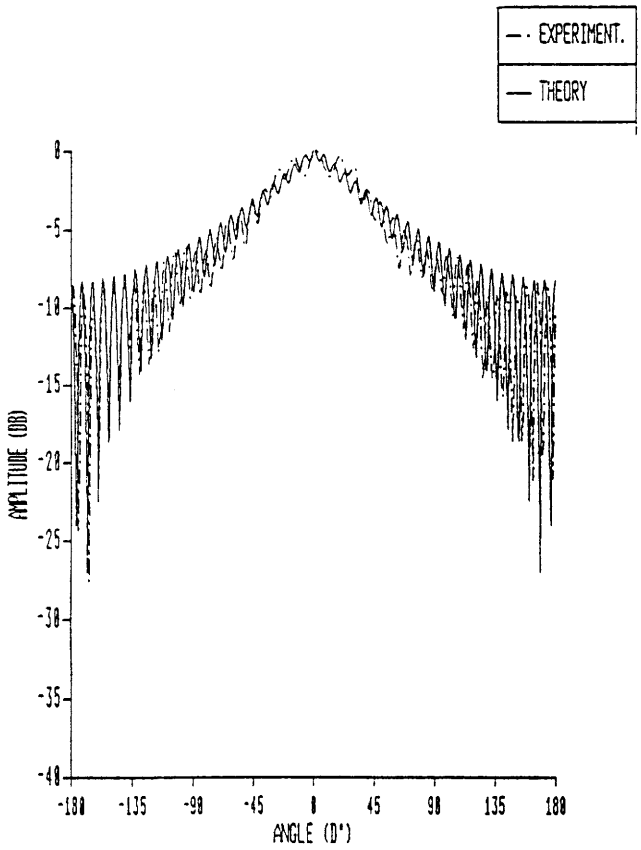

Figure 7 : slot on a truncated coated cone

The results are in good agreement. The introduction of a dielectric increases the levels of the oscillations in the shadow region : the creeping waves on the dielectric surface are guided and much less attenuated.

3 Coupling

3.1 Surface field

a) Theory

In the case of a circular cylinder, when the source O is at (ρ_o =a, ϕ_o, z_o) and the field point P at (ρ where $a \leq \rho \leq b$,ϕ,z), the scalar Green's function G is given by the integral expression (5.2) given in the appendix.

The residue method leads to the following expression of the Green's function :

$$G(\vec{\rho}, \vec{\rho_o}) \approx \frac{-j}{2\pi a} \sum_{n=o}^{+\infty} \sum_{p=-\infty}^{+\infty} \int_{-\infty}^{+\infty} \frac{R(\gamma_n)}{v_1} e^{-jh(z-z_o)} \; e^{-j\gamma_n |(\phi-\phi_o)+2\pi p|} \, dh \qquad (3.1)$$

$$R(\gamma_n) = \left\{ \frac{k_1\varepsilon_0}{k_0\varepsilon_1} \frac{\left(H_{\gamma_n}^{(2)'}(\nu_1 b)H_{\gamma_n}^{(1)}(\nu_1\rho) - H_{\gamma_n}^{(2)}(\nu_1\rho)H_{\gamma_n}^{(1)'}(\nu_1 b)\right)}{\left(H_{\gamma_n}^{(2)'}(\nu_1 b)H_{\gamma_n}^{(1)}(\nu_1 a) - H_{\gamma_n}^{(2)}(\nu_1 a)H_{\gamma_n}^{(1)'}(\nu_1 b)\right)} \frac{H_{\gamma_n}^{(2)}(\nu b)}{\left(\frac{\partial\left[H_\gamma^{(2)'}(\nu b) - j\, C_h(\gamma)H_\gamma^{(2)}(\nu b)\right]}{\partial\gamma}\right)_{\gamma=\gamma_n}} \right.$$
$$\left. + \frac{\left(H_{\gamma_n}^{(2)}(\nu_1\rho)H_{\gamma_n}^{(1)}(\nu_1 b) - H_{\gamma_n}^{(2)}(\nu_1\rho)H_{\gamma_n}^{(1)}(\nu_1 a)\right)}{\left(H_{\gamma_n}^{(2)'}(\nu_1 b)H_{\gamma_n}^{(1)}(\nu_1 a) - H_{\gamma_n}^{(2)}(\nu_1 a)H_{\gamma_n}^{(1)'}(\nu_1 b)\right)} \frac{H_{\gamma_n}^{(2)'}(\nu b)}{\left(\frac{\partial\left[H_\gamma^{(2)'}(\nu b) - j\, C_h(\gamma)H_\gamma^{(2)}(\nu b)\right]}{\partial\gamma}\right)_{\gamma=\gamma_n}} \right\}$$

where $\nu^2 = k_o^2 - h^2$ and $\nu_1 = \nu\sqrt{\varepsilon_r}$,

and γ_n is the n^{th} pole, root of the characteristic equation $H_{\gamma_n}^{(2)'}(\nu b) - j\, C_h(\gamma_n)H_{\gamma_n}^{(2)}(\nu b) = 0$

We introduce the parameter : $\gamma_n \approx \nu b + m_\nu \tau_n$ where $m_\nu = \left(\frac{\nu b}{2}\right)^{1/3}$. We note

$$b\,\left|(\phi - \phi_o) + 2\pi p\right| = s_p \cos\psi \text{ and } z - z_o = s_p \sin\psi$$

$$h = k_o \sin\alpha \text{ and } \nu = k_o \cos\alpha$$

So, the Green's function is written as :

$$G(\vec{\rho}, \vec{\rho_o}) \approx \frac{-j}{2\pi a\varepsilon_r} \sum_{n=0}^{+\infty} R(\gamma_n) \sum_{p=-\infty}^{+\infty} \int_{-\infty}^{+\infty} e^{-jk_o s_p \cos(\alpha - \psi)} d\alpha \; e^{-jm_\nu \tau_n \left|(\phi - \phi_o) + 2\pi p\right|} \tag{3.2}$$

Then, the stationnary phase method is applied to the integral. The first derivative of the exponential term is equal to zero for $\alpha_s = \psi_s$. Consequently,

$$G(\vec{\rho}, \vec{\rho_o}) \approx \frac{-j}{2\pi a\varepsilon_r} \sum_{p=-\infty}^{+\infty} \sum_{n=0}^{+\infty} R(\gamma_n)\sqrt{\frac{2\pi j}{k_o s_p}}\; e^{-jk_o s_p} \; e^{-jm_\nu \tau_n \left|(\phi - \phi_o) + 2\pi p\right|}$$

Introducing the following parameters :

$$\xi' = \frac{m_\nu s_p}{\rho_g} \text{ and } m_\nu = \left(\frac{\nu\rho_g}{2}\right)^{1/3}$$

where $\rho_g = \frac{b}{\cos\psi^2}$ is the radius of curvature in the principal plane (s^i,N,T) defined by the direction

of the incident ray, the normal and the binormal at the diffraction point and the Green's function $G(\vec{\rho}, \vec{\rho}_o)$ takes the following form :

$$G(\vec{\rho}, \vec{\rho}_o) \approx \sum_{p=-\infty}^{+\infty} \frac{1}{2\pi} \frac{e^{-jk_o s_p}}{s_p} v(\xi') \tag{3.3}$$

where
$$v(\xi') = e^{-j\pi/4} (\xi')^{1/2} \frac{1}{2\sqrt{\pi}} \frac{-j2\pi}{a\varepsilon_r} \sum_{n=0}^{+\infty} R(\gamma_n) \left(\frac{4\rho_g}{k_o^2}\right)^{1/3} e^{-j\xi'\tau_n} \tag{3.4}$$

Then, it is easy to extend the asymptotic expressions to the case of a general convex surface. We introduce the radius of curvature defined in the principal plane (ρ_g, ρ_t) ($\rho_t = \infty$ for the objects considered here) and we set :

$$\xi' = \int_{OP} \frac{v}{2m_v^2(\bar{s})} d\bar{s} = \int_{OP} \frac{m_v(t)}{\rho_g(t)} dt$$

The characteristic equation is modified : we introduce the principal radius of curvature ρ_1 (and ρ_2 if ρ_t is finite) as in the case of radiated fields. The poles-residues are roots of the modified characteristic equation :

$$H_\gamma^{(2)'}(k_o\rho_1 \sin\theta_n) - j\, C_h(\gamma)\, H_\gamma^{(2)}(k_o\rho_1 \sin\theta_n) = 0 \tag{3.5}$$

When the surface is convex, the radius of curvature at O and P are different. Consequently, the roots of the characteristic equation (or poles-residues) depend on the radius of curvature and must be calculated at each diffraction point. And (3.4) takes the following form :

$$v(\xi') = e^{-j\pi/4} (\xi')^{1/2} \frac{1}{2\sqrt{\pi}} \frac{-j2\pi}{a\varepsilon_r} \sum_{n=0}^{+\infty} R(\bar{\gamma}_n) \left(\frac{4\rho_g}{k_o^2}\right)^{1/3} e^{-j\xi'\bar{\tau}_n} \tag{3.6}$$

$\bar{\gamma}_n$ and $\bar{\tau}_n$ are determined from the introduction of a 'mean' radius of curvature $\bar{\rho}_1 = (\rho_1(O)\rho_1(P))^{1/2}$

b) Experimentation

An X-band slot is set on the perfectly conducting surface of the circular cylinder given in section 2.1,d. The results are obtained at $10GH_z$. (Figure 8) shows the surface field of the slot modelled by an infinite magnetic line source in the equatorial plane (θ=90°). The dielectric thickness is $\leq 0.1\lambda$: one mode and the two associated creeping waves are considered. The surface field is measured by mean of a probe moving very close to the surface, at a distance of about 3mm.

In the vicinity of the source, the differences between theory and experimentation are important. They are accentuated when the cylinder is coated by a dielectric : the creeping wave is guided on the dielectric surface and the differences between line and source are accentuated. In the shadow region, they are reduced. Consequently, the line model is interesting because of its simplicity as a tool in a first analysis of the phenomenon.

Since the dielectric thickness is $\leq 0.1\lambda$, it is possible to model the coated circular cylinder by a circular cylinder with a surface impedance [1] : the choosen surface impedance is the relative modal impedance of the first creeping wave propagation mode. (Figure 9) shows the validity of this theory. For a dielectric with thickness $> 0.1\lambda$, more than one mode is necessary to describe the propagation. So, it is impossible to define a surface impedance from these modes.

3.2 Coupling

a) Theory

The coupling between apertures set on a perfectly conducting surface with dielectric coating or not is an application of the surface field computation. So, longitudinal X-band slots are set on the conducting surface of a dielectric coated elliptic cylinder or truncated cone. We model these apertures by longitudinal magnetic dipoles. The mutual impedances or admittances are determined by means of the reaction theorem. The mutual admittance is determined considering only one mode of creeping waves and the two associated rays. The computation of the self admittance requires a particular development.

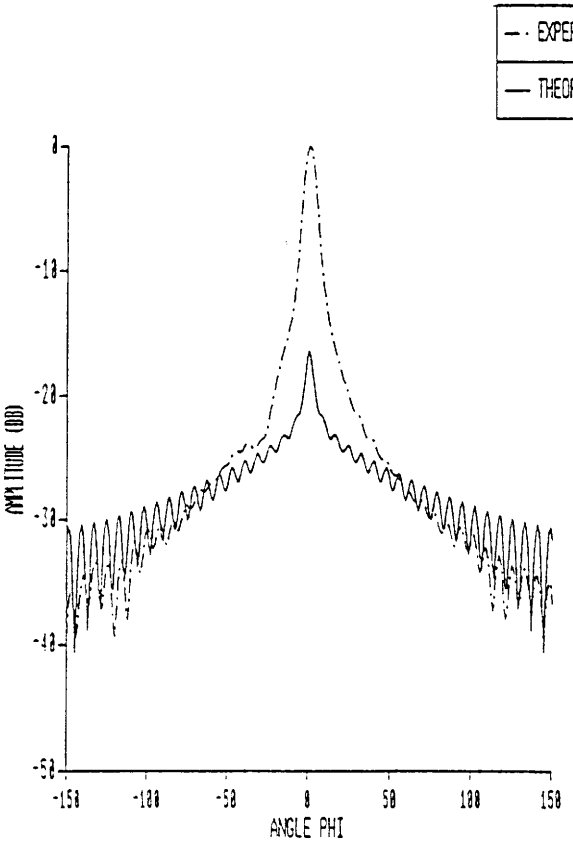

Figure 8 : surface field due to a magnetic line source on a coated circular cylinder

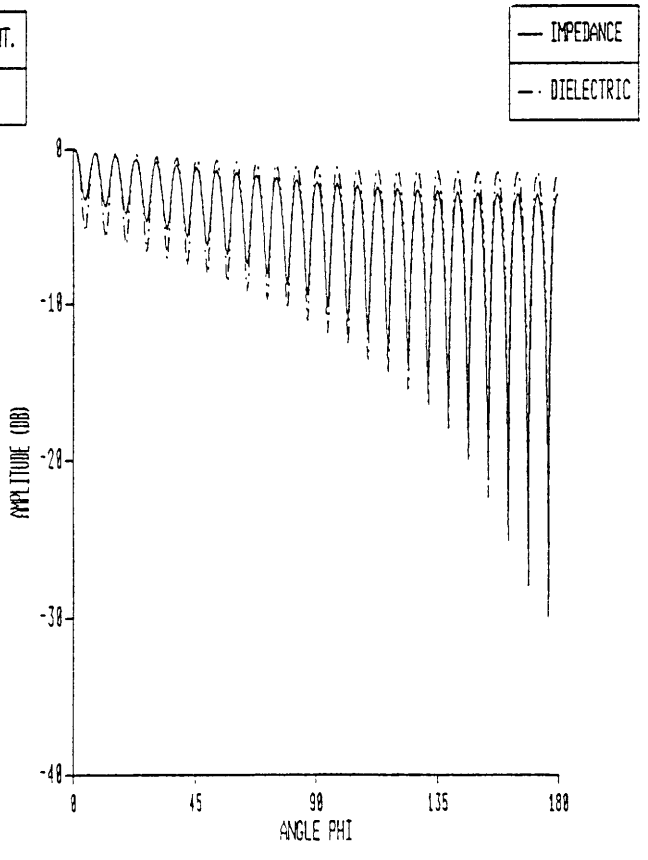

Figure 9 : surface impedance/dielectric

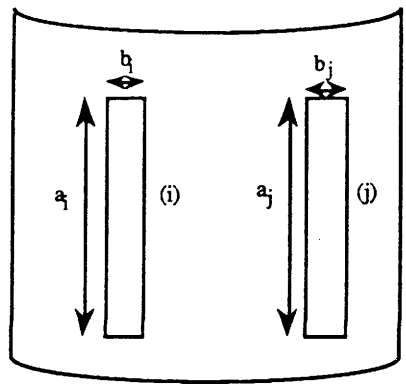

Figure 10 : slots on a convex surface

The expression for the self and mutual amittance of two arbitrarily located slots is derived from the reaction concept [2] and is given by

$$Y_{ij} = \iint_{s_j} \frac{(\mathbf{E}^j \Lambda \mathbf{H}^i) \cdot d\mathbf{s}_j}{V_i V_j}$$

We call : s_i the aperture (i), s_j the aperture (j), $\mathbf{H}^i$ the magnetic field when slot (i) is excited by a voltage V_i and the slot (j) is short circuited, $\mathbf{E}^j$ the electric field when slot (j) is excited by a voltage V_j and the slot (i) is short circuited. The aperture (i) dimensions are called $[a_i, b_i]$ and those of aperture (j) $[a_j, b_j]$ (Figure 10). The principal excitation mode is the TE_{10} mode. The longitudinal slots are in the equatorial plane (θ=90°).

Then, the mutual admittance is given by :

$$Y_{ij} = -\frac{8}{\pi^2}\sqrt{a_i b_i a_j b_j}\; C(b_i \sin\theta)\; C(b_j \sin\theta)\; S(a_i \sin\theta)\; S(a_j \sin\theta)\; g_z \qquad (3.7)$$

$$\text{with } S(X) = \frac{\sin(k_o X/2)}{(k_o X/2)} \text{ and } C(X) = \frac{\cos(k_o X/2)}{1 - (k_o X/\pi)^2}$$

$$g_z = G(k_o s)\, D\, v(\xi') \qquad G(k_o s) = \frac{k_o^2 Y_o}{2\pi j}\frac{e^{-jk_o s}}{k_o s}$$

D is the divergence factor defined in (2.2). The Fock function has been defined before.

The determination of the self admittance is not straightforward. The integral giving the self admittance is divergent. As in [5], in the vicinity of the source point, it is necessary to decompose the Green's function into two terms : a term giving the Green's function of an aperture set on the conducting surface of a coated perfectly conducting planar surface and a term which is the difference between the divergent term and the one relative to the plane. We use only the term corresponding to the plane, the surface being replaced by its tangent plane. When the conducting surface is coated with a dielectric, it is considered as a perfectly conducting one located in a medium with propagation constant $k_1 = k_o\sqrt{\varepsilon_r}$.

The coupling coefficient S_{ij} is given by :

$$S_{ij} = \frac{-2Y_G Y_{ij}}{(Y_G + Y_{ii} + Y_{ij})(Y_G + Y_{ii} - Y_{ij})} \qquad (3.8)$$

where Y_G is the characteristic admittance of the slot.

b) Exprimentation

Computations and measurements have been done at a frequency of 10 GH_z in the case of an elliptic cylinder (Figure 11) and a truncated cone (Figure 12) which are perfectly conducting and coated by a dielectric. The dielectric permittivity is (3.4,-0.1) and the tickness d=3 mm. The truncated cone has been described in 2.2.b, the X-band slots are set on the truncated cone at mid-height and separated by an angle of 45, 90, 135, 180°. The elliptic cylinder is defined by the half-length of its great axis A=150mm and the half-length of its small axis B=100mm. The slot (i) is set on the conducting surface at a distance A from the center of the cylinder and the slot (j) at a point on the surface making an angle of 45, 90, 135, 180° with respect to the great axis. One propagation mode and the two associated rays are sufficients because of the value of the dielectric thickness. The theoretical result agrees with the experimental ones. The introduction of a dielectric increases significantly the coupling between the apertures when the angular difference between apertures is > 45° (increase of 30 DB).

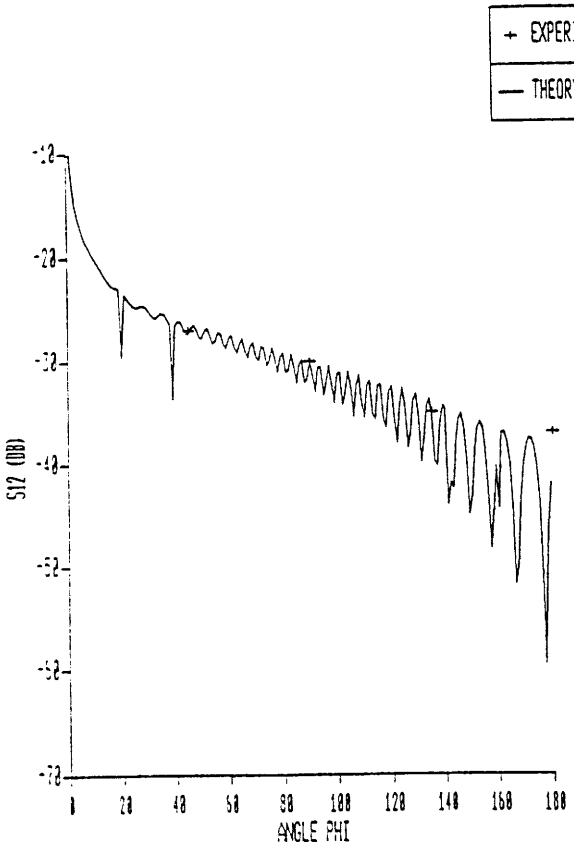

Figure 11 : coupling -elliptic cylinder-

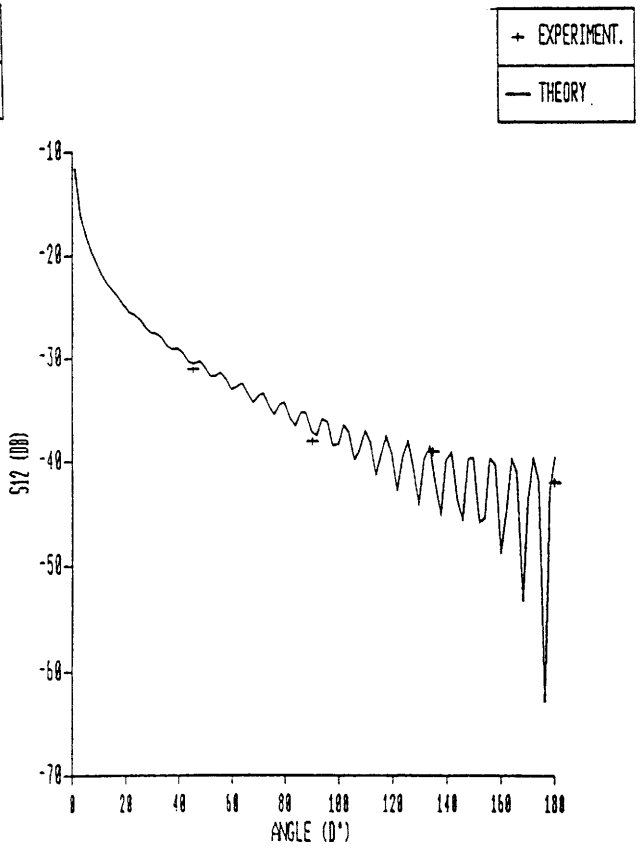

Figure 12 : coupling -truncated cone-

4 Conclusion

The numerical and experimental studies which have been presented, show the capabilities offered by the asymptotic methods to describe the radiation and the coupling between apertures set

on dielectric coated convex surfaces. We showed the utility of a simplified modelization for the slots (line source) as a first approach to analyze a difficult problem. Finally, the surface impedance approximation is introduced in a natural way when their coatings are considered. The methods can be generalizated to convex surfaces with finite radius of curvature and so permit to consider other surface singularities like edges or tips.

The method presented here does not require a large memory since there is no matrix needed and the computation of the fields requires the storage of few parameters. On the other hand, most part of the computer time is devoted to the computation of the roots of the characteristic equation which was done practically in real time. The computer was an IBM 3090.

5 Appendix

The transverse electric mode, called TE, is defined with respect to the z-axis, the generating line of the circular cylinder. We call G the Green's function which satisfies the Neumann's boundary condition on the conducting surface of the dielectric coated cylinder (TE). The electric or magnetic fields are obtained from the scalar Green's function.

dipole source and field points outside the dielectric :

$$G(\vec{\rho},\vec{\rho}_o) = \frac{-j}{8\pi}\int_{-\infty}^{+\infty} e^{-jh(z-z_o)} \left\{ \sum_{n=-\infty}^{n=+\infty} H_n^{(2)}(v\rho_>)\left(J_n(v\rho_<) - \frac{J_n'(vb) - j\,C_h(n)J_n(vb)}{H_n^{(2)'}(vb) - j\,C_h(n)H_n^{(2)}(vb)} H_n^{(2)}(v\rho_<)\right) e^{-jn(\phi-\phi_o)} \right\} dh \qquad (5.1)$$

with $v^2 = k_o^2 - h^2$

Relative modal impedance for the TE case :

$$C_h(n) = -j\frac{Z_1}{Z_o}\,\frac{H_n^{(1)'}(v_1b)H_n^{(2)'}(v_1a) - H_n^{(2)'}(v_1b)H_n^{(1)'}(v_1a)}{H_n^{(1)}(v_1b)H_n^{(2)'}(v_1a) - H_n^{(2)}(v_1b)H_n^{(1)'}(v_1a)} \quad \text{with} \quad v_1 = v\sqrt{\varepsilon_r}$$

Dipole source and field points inside the dielectric :

$$G(\vec{\rho},\vec{\rho}_o) = \frac{-j}{8\pi}\int_{-\infty}^{-\infty} e^{-jh(z-z_o)} \sum_{n=-\infty}^{n=+\infty} \frac{J_n(v_1\rho_<)Y_n'(v_1a) - J_n'(v_1a)Y_n(v_1\rho_<)}{J_n(v_1b)Y_n'(v_1a) - J_n'(v_1a)Y_n(v_1b)}$$
$$\left\{ \frac{k_1\varepsilon_o}{k_o\varepsilon_1}\left(J_n'(v_1b)Y_n(v_1\rho_>) - J_n(v_1\rho_>)Y_n'(v_1b)\right)\frac{H_n^{(2)}(vb)}{H_n^{(2)'}(vb) - j\,C_h(n)H_n^{(2)}(vb)} \right.$$
$$\left. + \left(J_n(v_1\rho_>)Y_n(v_1b) - J_n(v_1b)Y_n(v_1\rho_>)\right)\frac{H_n^{(2)'}(vb)}{H_n^{(2)'}(vb) - j\,C_h(n)H_n^{(2)}(vb)} \right\} e^{-jn(\phi-\phi_o)}\,dh \qquad (5.2)$$

with $a \le \rho_<, \rho_> \le b$ and $\rho_o = \rho_<$ and $\rho = \rho_>$ if $\rho_o \le \rho$ $\rho_o = \rho_>$ and $\rho = \rho_<$ if $\rho_o \ge \rho$ and $v_1 = v\sqrt{\varepsilon_r}$

dipole source and fields points in different media :

$$G(\vec{\rho},\vec{\rho_o}) = \frac{-j}{8\pi}\int_{-\infty}^{+\infty} e^{-jh(z-z_o)} \sum_{n=-\infty}^{n=+\infty} H_n^{(2)}(\nu\rho_>) \frac{J_n(\nu_1\rho_<)Y_n'(\nu_1 a) - J_n'(\nu_1 a)Y_n(\nu_1\rho_<)}{J_n(\nu_1 b)Y_n'(\nu_1 a) - J_n'(\nu_1 a)Y_n(\nu_1 b)}$$
$$\left(J_n(\nu b) - \frac{J_n'(\nu b) - j\,C_h(n)J_n(\nu b)}{H_n^{(2)'}(\nu b) - j\,C_h(n)H_n^{(2)}(\nu b)} H_n^{(2)}(\nu b)\right) e^{-jn(\phi-\phi_o)}\,dh \qquad (5.3)$$

with

$a \le \rho_< \le b$ and $\rho_> \ge b$ and $\rho_0 = \rho_<$ and $\rho = \rho_>$ if $\rho_0 \le \rho$, $\rho_0 = \rho_>$ and $\rho = \rho_<$ if $\rho_0 \ge \rho$

6 References

[1] M.-A. BLONDEEL-FOURNIER, "Antennes sur des structures métalliques recouvertes de diélectrique : contribution à l'analyse du rayonnement en Hautes-Fréquences", Université de Paris VI Pierre et Marie Curie, Ph.D. Dissertation, June 1990.

[2] V. A. FOCK,"Electromagnetic diffraction and propagation problems", New-York, Pergamon, 1965.

[3] K. E. GOLDEN, G. E. STEWART and D. C. PRIDMORE-BROWN,"Approximation techniques for the mutual admittance of slot antennas on metallic cones", I.E.E.E. Trans. Antennas Propagat.,vol. AP-22, pp. 43-48, Jan. 1974.

[4] M. HAMADALLAH, "Radiation pattern of square patch mounted diagonally on cylinder", Electronics Letters, Vol. 24, pp. 1321-1322, Oct. 1988.

[5] H. T. KIM, "High frequency analysis of EM scattering from a circular conducting cylinder with dielectric/ferrite coating", The Ohio State University, Dept. of Electrical Engineering Ph.D. Dissertation, 1986.

[6] S. W. LEE, E. YUNG and R. MITTRA, (june 1979), "G.T.D. solution of slot admittance on a cone or cylinder", Proc. I.E.E. , Vol. 126 n° 6, pp. 487-492.

[7] N. A. LOGAN, "General research in diffraction theory", Missiles and Space Div., Lockheed Aircraft Corp., Vol. 1, Rep. LMSD-288087 and Vol. 2, Rep. LMSD-288088, Dec. 1959.

[8] R. PAKNYS and N. WANG, "High-frequency surface field excited by a magnetic line source on an impedance cylinder", I.E.E.E. Trans Antennas Propagat., vol. AP-35 pp.293-298, March 1987.

[9] L. W. PEARSON, "A ray representation of surface diffraction by a multilayer cylinder", I.E.E.E. Trans. Antennas Propagat., vol. ap-35, no. 6, pp.698-707, June 1987.

[10] T.C.K. RAO and M.A.K. HAMID, "G.T.D. analysis of scattering from a dielectric-coated conducting cylinder", I.E.E. Proc., Vol. 127, June 1980.

[11] E.V. SOHTELL, "Microstrip patch antennas on cylindrical structures", JINA 86, Conference Proceedings, Nice, France, pp.216-220, 1986.

[12] J. R. WAIT, "Electromagnetic radiation from cylindrical structures" , Pergamon Press, New-York, 1959.

[13] N. WANG, "Regge poles, natural frequencies and surface wave resonance of a circular cylinder with a constant surface impedance", I.E.E.E. Trans. Antennas Propagat., Vol. AP-30, pp. 1244-1247, Nov. 1982.